

Material Matters[™] **BASICS**

Volume 4

Fundamentals of Organic
Thin Film Solar Cells

AN ALDRICH[®] MATERIALS SCIENCE TUTORIAL

Introduction

In recent years, while global environmental and energy conservation issues have become increasingly serious, organic thin film solar cells have started to draw widespread attention from the public as a new energy source. Development of high-performance organic thin film solar cells (Figure 1, page 1) that can generate power at low cost is essential for global adoption of solar cells. Recently, the power conversion efficiency (PCE) of solar cells has rapidly improved and is approaching a level that will enable widespread use. This article presents an outline of the history and current status of the development of organic thin film solar cells. It then describes the power conversion mechanism in organic thin film solar cells and a method for fabricating organic thin film solar cell devices. The article also introduces a process for synthesizing fullerene derivatives.

Table of Contents

Fundamentals of Organic Thin Film Solar Cells

| | |
|--|---|
| Present Status of Organic Thin Film Solar Cells | 1 |
| History of Development of Organic Thin Film Solar Cells | 1 |
| Mechanism of Photoelectric Conversion in Organic Thin Film Solar Cells | 3 |
| Example of Strategy for Improving Power Conversion Efficiency | 3 |
| Process of Synthesizing Fullerene Derivatives | 4 |
| Method for Fabricating Organic Thin Film Solar Cells | 6 |
| Evaluation of Device Characteristics | 7 |
| Conclusion | 8 |
| Acknowledgments | 8 |

Featured Products

| | |
|--|----|
| P-type Organic Semiconductors | 10 |
| N-type Organic Semiconductors | 15 |
| PEDOT:PSS | 19 |
| Indium Tin Oxide (ITO) Coated Substrates | 19 |

Material Matters™ BASICS

Volume 4

**Aldrich Materials Science
Sigma-Aldrich Co. LLC**
6000 N. Teutonia Ave.
Milwaukee, WI 53209, USA

To Place Orders

Telephone 800-325-3010 (USA)
FAX 800-325-5052 (USA)

International customers, contact your local Sigma-Aldrich office (sigma-aldrich.com/worldwide-offices).

Customer & Technical Services

Customer Inquiries 800-325-3010
Technical Service 800-325-5832
SAFC® 800-244-1173
Custom Synthesis 800-244-1173
Flavors & Fragrances 800-227-4563
International 314-771-5765
24-Hour Emergency 314-776-6555
Safety Information sigma-aldrich.com/safetycenter
Website sigma-aldrich.com
Email aldrich@sial.com

Subscriptions

Request your FREE subscription to *Material Matters*™:

Phone 800-325-3010 (USA)
Mail Attn: Marketing Communications
Aldrich Chemical Co., Inc
Sigma-Aldrich Co. LLC
P.O. Box 2060
Milwaukee, WI 53201-2060
Website aldrich.com/mm
Email sams-usa@sial.com

Material Matters™

Explore online editions
of *Material Matters*™ aldrich.com/materialmatters



Now available for your iPad®
aldrich.com/mm

FUNDAMENTALS OF ORGANIC THIN FILM SOLAR CELLS

Yutaka Matsuo

Project Professor at School of Science, The University of Tokyo
Email: matsuo@chem.s.u-tokyo.ac.jp

Present Status of Organic Thin Film Solar Cells

The production of solar cells and the size of the solar cell market have expanded dramatically since the beginning of this century. However, the silicon-based solar cells that are now the main type in use require high production costs, so their widespread use is not possible without governmental subsidy. Accordingly, the fundamental issue of cost remains to be solved. To find a solution to this issue, research and development of new solar cells is actively conducted globally. The organic thin film solar cell (Figure 1) is one new type of solar cell that uses organic semiconductors, which are expected to become inexpensive in the future, instead of silicon semiconductors. Organic thin film solar cells have the characteristics of being lightweight and flexible. Therefore, if they become available for commercial use, a wide variety of new applications for solar cells, such as mobile battery chargers, will become accessible. In addition, when highly efficient long-life organic thin film solar cells are implemented in the future, we will be able to use them for photovoltaic power generation. This application will make it possible to increase the ratio of natural sources to fossil fuels used in energy production, resulting in a reduction in environmental loads and the amount of carbon dioxide emissions. However, the power conversion efficiency of conventional organic thin film solar cells is about 8% at a maximum, which is not comparable with the 10% of amorphous silicon solar cells and the 15 to 20% of polycrystal and single-crystal silicon solar cells. Through discussion and improvement, various efforts are being made towards the higher stability of organic materials and the longer life of organic thin film solar cells.

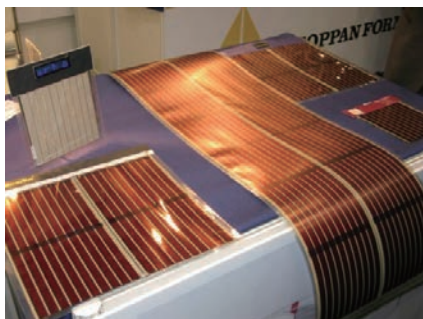


Figure 1. Organic Thin Film Solar Celles (Konarka Technologies).
Photo presented by Nikkei Electronics.

Historical Development of Organic Thin Film Solar Cells

In 1986, C. W. Tang of Eastman Kodak Company reported a prototype of an organic thin film solar cell.¹ This prototype was a heterojunction (p - n junction) solar cell in which an organic electron donor (organic p -type semiconductor) and an organic electron acceptor (organic n -type semiconductor) were joined together (Figure 2). Copper(II) phthalocyanine (Aldrich Prod. No. 702854) was used as the electron donor, and PTCBI (3,4,9,10-perylenetetracarboxylic bis-benzimidazole), a perylene diimide derivative, was used as the electron acceptor in the solar cell. This research was published the year after the discovery of fullerene C_{60} (Aldrich Prod. Nos. 572500, 379646, and 483036),² which had not yet been isolated. The photoelectric energy conversion significantly increased from that of conventional Schottky organic thin film solar cells to the 1% level when a single organic layer was used.³ This marked the first milestone breakthrough. Research on higher-efficiency p - n devices of this type, however, did not rapidly advance for several reasons, including the fact that Tang, the very developer of the prototype, subsequently focused on the research and development of organic electronic devices.⁴ In 1991, Hiramoto et al. reported on a p - i - n type device,⁵ which had an i -layer formed by codeposition of an electron donor and an electron acceptor between a p -layer and an n -layer. This device exhibited a conversion efficiency of only a little less than 1%. However, a bulk heterojunction, where an electron donor and an electron acceptor interblend, was formed in the i -layer, so this research was pioneering in the sense that it revealed the usability of bulk heterojunctions in organic thin film solar cells.

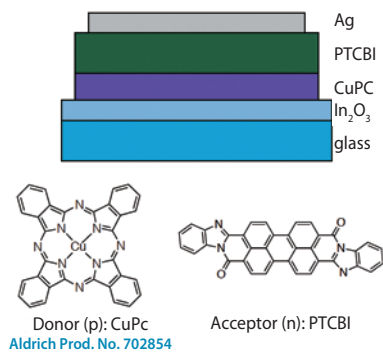


Figure 2. p - n Heterojunction Organic Thin Film Solar Cell.

In 1992, immediately after the synthesis and isolation⁶ of fullerenes had been developed, N. S. Sariciftci et al. showed a fullerene to be an excellent electron acceptor by revealing ultrafast charge separation (60 ns or less, which was the then limit of detection) from MEH-PPV (2-methoxy-5-(2-ethylhexyloxy)polyphenylenevinylene; **Figure 3; Aldrich Prod. No. 536512**, etc.), an electron-donating conductive polymer, to a fullerene (C_{60}).⁷ Yoshino et al. also independently examined the optical dynamics of a mixed film of a π -conjugated polymer and C_{60} .⁸ These research results can be considered as a second breakthrough. The speed of charge separation from a conductive polymer to a fullerene derivative was revealed to be about 45 fs as reported in 2001 after suitable measurement instrumentation had been developed.⁹

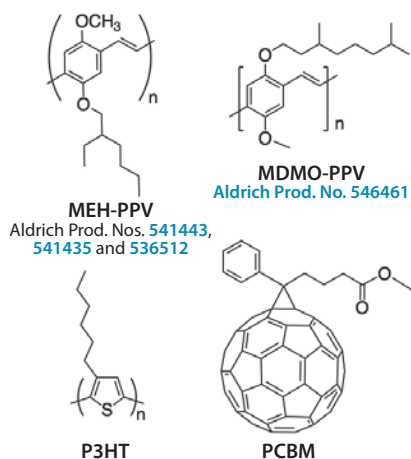


Figure 3. Conductive polymer materials and fullerene derivative used for organic thin film solar cells.

During this period, however, the PCE of organic thin film solar cells did not increase from the 1% reported in 1986, largely due to challenges related to the processing of fullerenes. The fullerenes, which exhibited low solubility in organic solvents, were not able to be dissolved at high concentrations in electron donor polymers. In 1995, the third breakthrough was made by A. J. Heeger et al.,¹⁰ that is, the advent of a soluble fullerene derivative and the use of a bulk heterojunction forming a charge separation layer in which a conductive polymer and a fullerene derivative were interblended. Substituting PCBM (phenyl C_{61} -butyric acid methyl ester; **Figure 3; Aldrich Prod. No. 684457**),¹¹ developed by J. C. Hummelen and F. Wudl et al., for C_{60} enabled the preparation of the MEH-PPV:PCBM = 20%:80% blend solution, which thereby made it possible to optimize the ratio of the electron donor to the electron acceptor. In addition, the use of a bulk heterojunction layer in which an electron donor and an electron acceptor are interblended made the area of the charge separation interface (the interface between the electron donor and the electron acceptor) wider than that of a heterojunction layer and formed a mixed layer with phase separation in the order of tens of nanometers. These advantages made it possible for excitons to reach the charge separation interface effectively. Excitons are pairs of negative and positive charges. Since each of the pairs can be considered to be a combination between the presence of an electron in the lowest unoccupied molecular orbital (LUMO) level and the absence of an electron in the highest occupied molecular orbital (HOMO) in a molecule, the excitons may also be regarded as organic molecules in an excited state. It is known that the distance (the diffusion length of the excitons) across which the excited state can propagate in an organic solid ranges from several nanometers to tens of nanometers. An organic thin film solar cell with a power conversion efficiency of 1.5% was thus fabricated using the MEH-PPV:PCBM blend. In 2001, a device with a power conversion efficiency of 2.5% was fabricated by substituting MDMO-PPV (**Figure 3; Aldrich Prod. No. 546461**) for MEH-PPV to optimize organic thin film morphology that differed depending upon the solvent used.⁹

Following this, researchers began examining the use of polythiophene as an alternative electron donor to PPV. In the beginning, this attempt did not work well, but, in 2002, C. J. Brabec reported achieving a PCE of 2.8% by combining poly-3-hexylthiophene (P3HT) (**Figure 3; Aldrich Prod. No. 698989**, etc.) with PCBM (**Aldrich Prod. No. 684457**, etc.).¹² Since this report, the race to develop P3HT:PCBM organic thin film solar cells has intensified in many countries. Significant power conversion efficiency changes depending upon the treatment after the fabrication of the device (post-treatment), and various post-treatment effects have been reported. In 2003, N. S. Sariciftci et al. (Johannes Kepler University of Linz, Austria) reported the acceleration of polymer crystallization by thermal annealing or application of an external voltage and using this to achieve a power conversion efficiency of 3.5%.¹³ In 2005, Y. Yang et al. (UCLA, USA) achieved a power conversion efficiency of 4.5% by annealing at 110 °C for 10 minutes.¹⁴ In the same year, D. L. Carroll et al. (Wake Forest University, USA) reported that the optimal annealing temperature and period were 155 °C and 5 minutes, respectively, and that they had implemented a device exhibiting a power conversion efficiency of 4.9%.¹⁵ In 2006, D. D. C. Bradley (Imperial College, United Kingdom) investigated the influence of regioselectivity of polythiophene on thin film morphology and photoelectric conversion characteristics in detail and reported on a device with a PCE of 4.4%.¹⁶ Subsequent reports of power conversion efficiencies ranging from the 4% level to those a little less than 5% led to the P3HT-PCBM combination becoming the standard material for organic thin film solar cells. The background of the progress from the combination of copper phthalocyanine and perylene diimide to that of PPV and C_{60} and on to that of P3HT-PCBM enables us to see that the optimization and improvement of the electronic characteristics and molecular assembly forming ability of molecules played significant roles in the improvement of the characteristics of organic thin film solar cells.

Since the establishment of the P3HT:PCBM standard device in around 2006, development of new materials has further boosted conversion efficiency (5–6%). Electron donors that can absorb long-wavelength light due to charge transfer absorption in molecules were developed by incorporating an electron-deficient unit into a π -conjugated polymer (**Figure 4**).^{17–19} In addition, fullerene bisindene adducts with 56 π -conjugated systems were developed as electron acceptors by further scaling down the conjugated systems of fullerenes.^{20–23} The fullerene bisindene adducts have a high LUMO level and provide a high open circuit voltage (V_{oc}). Moreover, research on device structure has led to developments such as tandem construction,²⁴ in which solar cells are connected in series, and the optical spacer²⁵ for absorbing light reflected on its rear electrode efficiently by its active layer.

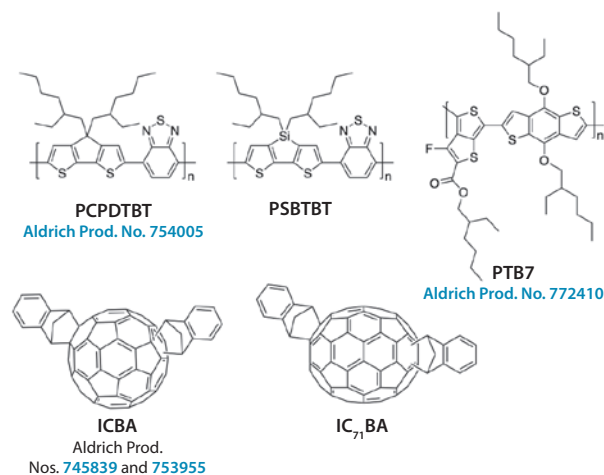


Figure 4. Narrow band gap polymers and high LUMO fullerene derivatives.

Mechanism of Photoelectric Conversion in Organic Thin Film Solar Cells

This section describes how organic thin film solar cells convert solar energy into electrical energy. The photoelectric conversion mechanism in organic thin film solar cells is shown using a typical example of a *p-n* type device in **Figure 5**. Incident light reaching an organic thin film solar cell is absorbed chiefly by electron donor molecules, which are excited and produce excitons. These excitons diffuse to the interface between the electron donor and the electron acceptor, where electrons flow from the electron donor to the electron acceptor to form a charge separation state. In other words, the electron donor turns into cations (holes) by providing electrons for the electron acceptor, whereas the electron acceptor becomes anions by receiving those electrons. The holes flow toward the transparent electrode substrate, the electrons flow toward the counter electrode, and thus, the solar cell provides a current for an external circuit.

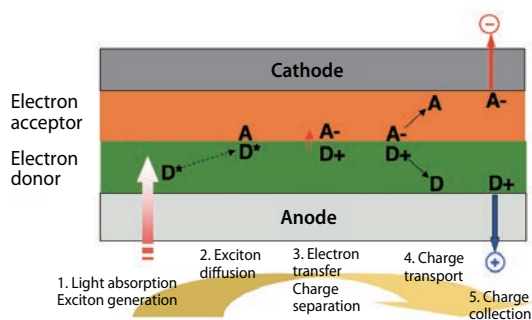


Figure 5. Mechanism for photoelectric conversion in organic thin film solar cells.

The mechanism for this photoelectric conversion can also be described by using an energy diagram (**Figure 6**). An electron donor molecule is excited to induce an electron present in the HOMO to rise to the LUMO; the electron flows downward in the energy diagram smoothly without encountering any barrier. Since the LUMO of the electron acceptor can accommodate an electron more stably, the raised electron transfers from the LUMO of the electron donor to the LUMO of the electron acceptor to form a charge separation state. In this state, the HOMO of the electron donor has a vacancy (which means that a hole is present), and the LUMO of the electron acceptor is occupied by an electron. The former is a radical cation, and the latter is a radical anion.

At this point, a larger HOMO-LUMO gap between the HOMO of the electron donor and the LUMO of the electron acceptor tends to produce a higher V_{oc} of the organic thin film solar cell. However, if the LUMO levels of the electron donor and electron acceptor are too close, it makes it difficult to form sufficient charge separation. At this stage, a difference in the order of 0.2 to 0.3 eV is required. A hole moves upward in the energy diagram smoothly without encountering any barrier, flowing from an electron donor molecule to the indium tin oxide (ITO) electrode, whereas an electron is collected by the aluminum electrode. Light induces electrons to flow within the solar cell from the ITO electrode with a high work function to the aluminum electrode with a low work function, enabling the solar cell to provide a current for an external circuit.

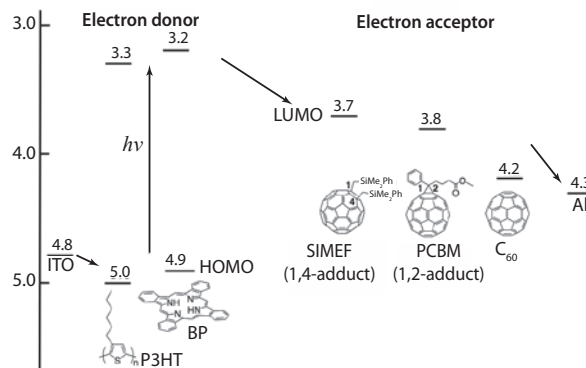


Figure 6. Energy diagram of organic thin film solar cell.

Example of Strategy for Improving Power Conversion Efficiency

Improvement of several factors contributes to an increase in power conversion efficiency. In this section, two areas for improvement are taken as examples from the point of view of material development. One of them is development of electron acceptor materials. Organic semiconductors have π -conjugated systems as their fundamental framework. Many of the π -conjugated compounds that hold π -conjugated planes possess a large number of π -electrons and usually act as electron donors. Almost all of the π -conjugated compounds obtained by expanding conjugated systems may become electron donors. This characteristic gives us the ability to tune a number of properties, so research on these materials has been advancing. On the other hand, to obtain an electron acceptor, the energy level must be modified by bending π -conjugated systems or reducing π -electron density with the aid of electron-withdrawing groups. Fullerenes, which have π -conjugated systems that are bent and connected to form closed spherical shapes, are optimal as electron acceptors. Fullerene C_{60} itself is disadvantaged in that it takes only low voltage because its electron affinity is too high. Accordingly, fullerene derivatives obtained by chemical synthesis in which organic groups are attached to fullerenes are used for organic thin film solar cells. However, selective chemical modification of fullerenes is not easy, and it is costly to separate a desired fullerene product from a given mixture to highly purify it. In fact, typically only PCBM is used as electron acceptors in this research field at the present, providing only limited choices. Another area for improvement is construction of the structure between the electron donors and electron acceptors. Currently, the method of constructing a bulk heterojunction by spin coating a blend solution of an electron donor and an electron acceptor is frequently applied for depositing two materials in an organic thin film (**Figure 7**). However, it is difficult to fabricate the desired structure by using this method, and directing our efforts into constructing ideal phase separation structures has become increasingly important. A structure in which electron donors and electron acceptors are incorporated alternately (**Figure 7**) is thought to be optimal for charge separation and charge transfer.

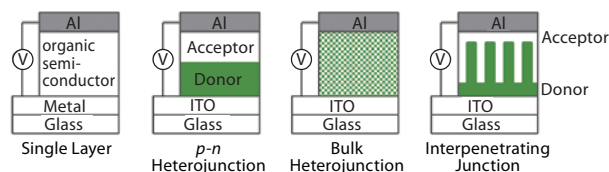


Figure 7. Various device structures of organic thin film solar cells.

Process of Synthesizing Fullerene Derivatives

The opto-electronic function of fullerene derivatives is brought about by the π -conjugated systems that are bound to the fullerene frameworks. The shape of π -conjugated systems changes depending on the number and positions of organic groups that are added to the fullerenes. In other words, the development of a process for introducing the desired number of organic groups at the desired positions would make it possible to design π -conjugated system structures that optimize the opto-electric function. Based on such ideas, a variety of fullerene derivatives with various π -conjugated systems have been synthesized (Figure 8). This chapter describes the methods for synthesizing typical fullerene derivatives.

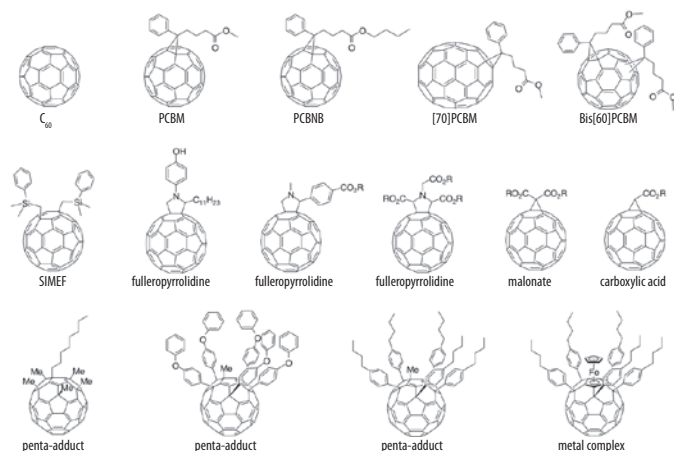


Figure 8. Various fullerene derivatives.

Synthesis of PCBM

[60]PCBM (Phenyl C_{61} -Butyric acid Methyl ester, Aldrich Prod. Nos. 684457, 684449, and 684430) is the most frequently used electron acceptor. Tosylhydrazone, which is storable, is synthesized in advance and used in the reaction with C_{60} (Figure 9). In the reaction of synthesizing PCBM, a base abstracts hydrogen atoms to produce diazoalkane $PhC(=N_2)CH_2CH_2CH_2CO_2Me$, which is decomposed to generate carbene. This carbene is added to C_{60} to produce a derivative. In the beginning, a [5,6] adduct forms as a kinetically obtained product. Heating this product at a high temperature yields PCBM, a [6,6] adduct that is a thermodynamic product usually used as an electron acceptor. The following is the procedure for the reaction.¹¹ Recently, the following materials have also often been used: PCBM with different lengths of alkyl groups in their side chains; [70]-PCBM (Aldrich Prod. No. 684465), which is a derivative of C_{70} ; and Bis[60]PCBM (Aldrich Prod. No. 704326), which is known for producing a high open circuit voltage.

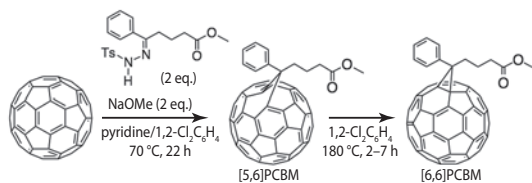


Figure 9. Synthesis of PCBM.

Procedure for Synthesis of Methyl 4-Benzoylbutyrate *p*-Tosylhydrazone

Methyl 4-benzoylbutyrate (20.6 g, 0.1 mol) and *p*-toluenesulfonylhydrazide (22.3 g, 1.2 equiv; Aldrich Prod. No. 132004) are heated to reflux in methanol (70 mL) for 5.5 hours. Subsequently, the reaction mixture is left without heating for one day and then cooled to $-15\text{ }^\circ\text{C}$. The mixture is filtrated to obtain the resulting crystal, which is then rinsed in a small amount of cooled methanol. Finally, the crystal is dried in a desiccator, and 35.9 g of the product is obtained as a white crystal (yield: 96%).

Procedure for Synthesis of PCBM (in a nitrogen gas flow)

Methyl 4-benzoylbutyrate (1.50 g, 4 mmol) is put into a three-necked flask equipped with a nitrogen gas inlet, a thermometer, and a magnetic stirrer and dissolved in dried pyridine (30 mL). NaOMe (225 mg, 4.16 mmol) is added to the mixture, and the mixture is stirred for 15 minutes. A solution of C_{60} (1.44 g, 2 mmol; Aldrich Prod. No. 572500) in 1,2-dichlorobenzene (100 mL) is added to the mixture, and then the reaction is allowed to progress in the mixture at a temperature of 65 to 75 $^\circ\text{C}$ for 22 hours. The progress of the reaction can be followed by using a TLC plate (SiO_2 /toluene). The reaction mixture is put into a round flask and condensed under reduced pressure (about 0.1 mm Hg) until its total volume is reduced to 70 mL. This solution is put into a silica gel column with a mobile phase of toluene and then developed to batch off the product, first with a mobile phase of chlorobenzene (100 mL) and subsequently with a mobile phase of chlorobenzene-toluene solution with toluene gradually increased. The first band is unreacted C_{60} . The obtained solution of the product undergoes vacuum concentration until its volume is reduced to 20 mL, and then diethyl ether is added to the solution to perform reprecipitation. The product is filtrated to obtain the purified solid, which is then rinsed in a small amount of diethyl ether. Finally, the solid is dried at 70 $^\circ\text{C}$ under reduced pressure, and 837 mg of PCBM is obtained (yield: 58%). The product thereby obtained is a [5,6] adduct. The product is dissolved into 1,2-dichlorobenzene (concentration: 1.5 to 10 mg/mL) and then heated to reflux at 180 $^\circ\text{C}$ for 2 to 7 hours to isomerize it, yielding PCBM, a [6,6] with a yield of 98%.

Synthesis of SIMEF

SIMEF is a possible substitute for PCBM as an electron acceptor.^{26,27} This section describes the characteristics of SIMEF and a method for synthesizing it. We developed a fullerene derivative $C_{60}(CH_2SiMe_2R)_2$ (where R can be various organic groups; Figure 11) with two substituted silylmethyl groups. This fullerene derivative has the following characteristics: (a) electronic characteristics that produce high voltage; (b) a packing structure consisting of aligned fullerenes that are able to produce large current; and (c) a thermal crystallization behavior that enables crystallization in thin films. For easier pronunciation, we named this series of fullerene derivatives with silylmethyl groups SIMEF (sai-mef), an abbreviation of silylmethylfullerene. In particular, a simple representation of SIMEF refers to a bis-phenyl derivative $C_{60}(CH_2SiMe_2Ph)_2$ useful as a standard material for electron acceptors. Substituents on the silicon atoms can be easily replaced in SIMEF. This is because the formation of carbon-silicon bonds is easier than that of carbon-carbon bonds in synthetic organic chemistry. This gives SIMEF its versatility, enabling precise design of the packing structure and electronic characteristics.

SIMEF, which possesses 1,4-type 58 π -electron systems, has a higher LUMO level and so affords a high open circuit voltage compared to PCBM, which possesses 1,2-type 58 π -conjugated systems (Figure 6). In addition, the thermal crystallization behavior of SIMEF is especially important. SIMEF is transformed at 150 °C from an amorphous solid to a crystalline solid that reflects X-ray diffraction measurement. In this crystalline solid, C_{60} parts in SIMEF are aligned in straight columnar arrays (Figure 10). This structural change can be regarded as a kind of phase separation. In other words, C_{60} parts have a tendency to aggregate with one another, and organic groups in the side chains aggregate with one another, so that such a structure forms. The pores of the distorted honeycomb-like hexagonal lattice formed by C_{60} parts are occupied by organic groups. It is thought that this structure enables electrons to efficiently flow into the aligned C_{60} parts. SIMEF exhibits relatively high mobility as an *n*-type organic semiconductor: 5.8×10^{-2} cm²/Vs (FET; field-effect transistor) and 8.0×10^{-3} cm²/Vs (SCLC; space-charge limited current).

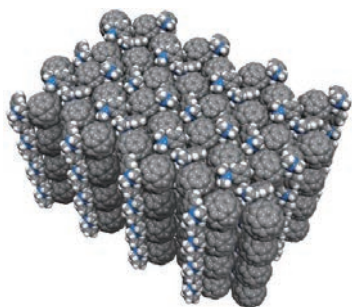


Figure 10. Crystal packing structure of SIMEF.

SIMEF is synthesized by nucleophilic addition reaction of fullerenes with nucleophilic reagents and the nucleophilic substitution reaction between fullerene anions and alkyl halides (Figure 11).²⁶ At first glance, the key addition reaction of organometallic reagents to fullerenes seems simple, but in fact it is not. This is because electron transfer occurs between a RC_{60}^- and a starting material C_{60} present in the system. In the course of pursuing a highly efficient mono-addition reaction, we discovered the fact that the silylmethyl anion is an excellent carbon nucleophile in the nucleophilic addition reaction with fullerenes and that the addition of dimethylformamide (DMF) remarkably accelerates this nucleophilic addition reaction. By using this discovery, we developed a highly efficient reaction to produce mono-adducts. We think that the efficiency of this reaction is enhanced by the following two processes. DMF coordinates to magnesium atoms in the Grignard reagent to improve the reactivity of the Grignard reagent. DMF coordinates further to magnesium atoms in the intermediate complex, MgC_{60} to stabilize it.

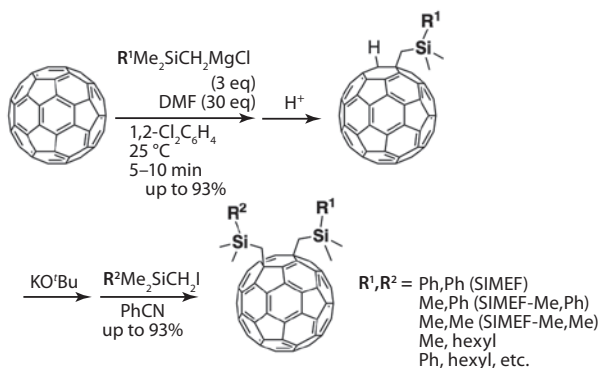


Figure 11. Synthesis of SIMEF.

Procedure for Synthesis of Mono-adduct $C_{60}(CH_2SiMe_2Ph)H$

C_{60} (2.00 g, 2.78 mmol), *N,N*-dimethylformamide (6.45 mL, 83.3 mmol), and 1,2-dichlorobenzene (500 mL) are put into a 1 L three-necked flask under a nitrogen atmosphere. A THF solution of $PhMe_2SiCH_2MgCl$ (0.85 M, 9.80 mL, 8.33 mmol) is dropped into this mixture at 25 °C. The mixture is stirred for 10 minutes, and then saturated ammonium chloride aqueous solution (1.0 mL) is added to the mixture to terminate the reaction. After the solvent is distilled away under reduced pressure, the residue is dissolved in toluene (200 mL), and then this solution is filtrated with a silica gel short column to remove insoluble matter. The filtrate undergoes vacuum concentration in an evaporator until its volume is reduced to about 5 to 10 mL, and then methanol (100 to 200 mL) is added to the filtrate to perform reprecipitation. After preparative HPLC isolation and purification (Buckyprep column; toluene/2-propanol = 7/3) of the resulting brown powder, the analytically pure target product is obtained in 82% yield (1.99 g, 2.28 mmol).

Procedure for Synthesis of Bis-adduct $C_{60}(CH_2SiMe_2Ph)_2$ (SIMEF)

$C_{60}(CH_2SiMe_2Ph)H$ (1.02 g, 1.17 mmol) is dissolved in benzonitrile under nitrogen. A THF solution of potassium *t*-butoxide (1.0 M, 1.41 mL, 1.41 mmol; Aldrich Prod. No. 328650) is dropped into the solution at 25 °C. After the solution is stirred for 10 minutes, $PhMe_2SiCH_2Cl$ (4.23 mL, 23.4 mmol) and potassium iodide (23.4 mmol; Aldrich Prod. No. 429422) are added to the solution. The solution is stirred at 110 °C for 17 hours, and then cooled to room temperature. After the solvent is distilled away in reduced pressure, the residue is dissolved in toluene (100 mL), and then filtrated with a silica gel short column to remove insoluble matter. After vacuum concentration of the filtrate in an evaporator until its volume is reduced to about 2 to 5 mL, methanol (50 to 100 mL) is added to the filtrate to perform reprecipitation. The resulting dark brown powder is subjected to silica gel column chromatography (carbon disulfide/hexane = 1/1 to 1/5) or HPLC preparative isolation and purification (Buckyprep column; toluene/2-propanol = 7/3), so that the analytically pure target product is obtained as a black solid in 76% yield (0.906 g, 0.889 mmol).

Synthesis of Fulleropyrrolidine

Fulleropyrrolidine,²⁸ a compound that was reported soon after the research on the synthesis of fullerene derivatives had started, is sometimes used in organic thin film solar cells. Its synthesis is easy and can be produced by using readily available starting materials, commercially-produced *N*-methylglycine (Aldrich Prod. No. 131776) and paraformaldehyde. The reaction between the two starting compounds generates a five-membered lactone, which is then decomposed by heating into azomethine ylide, a 1,3-dipole compound (Figure 12). This azomethine ylide is added to a fullerene to produce fulleropyrrolidine. In the actual reaction, C_{60} , *N*-methylglycine, and paraformaldehyde are heated in toluene for 2 hours to reflux.

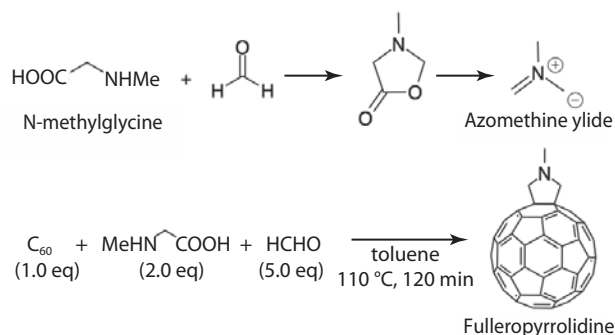


Figure 12. Synthesis of fulleropyrrolidine.

Method for Fabricating Organic Thin Film Solar Cells

This section describes a procedure for fabricating a typical organic thin film solar cell, a bulk heterojunction device (**Figure 13**) using P3HT and PCBM. This device, a standard building block of today's solar cell products, is fabricated by using a coating process; its anode is a transparent electrode substrate consisting of glass on which ITO is deposited, and its hole transport layer is made of PEDOT:PSS. **Figure 14** shows the flowchart of the procedure for fabricating the device.

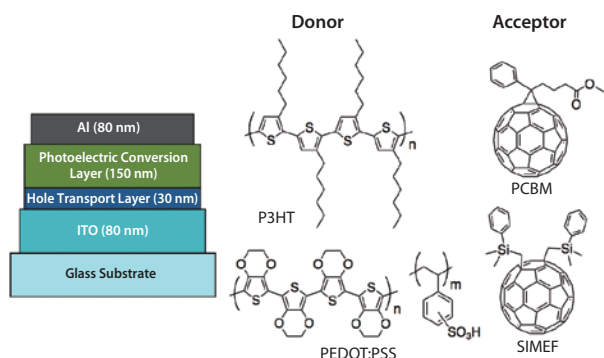


Figure 13. Device structure of Glass/ITO/PEDOT:PSS/P3HT/Acceptor/Al.

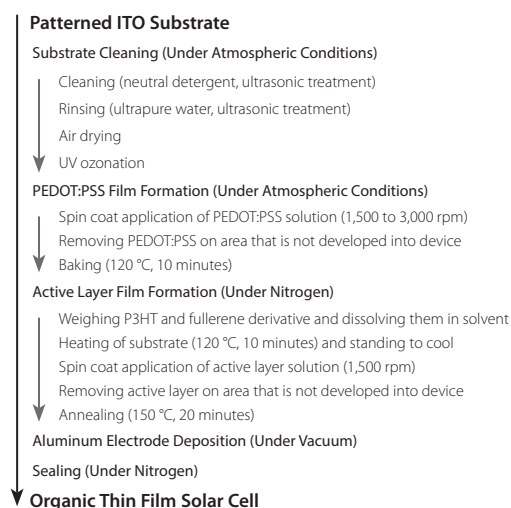


Figure 14. Flowchart of procedure for fabricating device.

Procedure for Fabricating Devices

Substrate Cleaning

ITO glass substrates with low surface resistance (about 10 Ω/sheet) for organic electroluminescence devices and solar cells are commercially available (aldrich.com/substrates). To form a photoelectric conversion layer on the substrates, which enables devices to function without a short circuit, it is desirable that their surfaces be as flat as possible (average surface roughness: Ra < 1 nm). The choice of substrate size varies, we used ITO glass slides (75 mm long, 25 mm wide, and 0.7 mm thick). The ITO had undergone patterning, so that the 2 mm × 2 mm device area has an electrode leading portion. **Figure 15** shows an example of patterning.

1. The ITO glass substrate surface is immersed in a solution obtained by diluting a commercially available neutral detergent for organic EL substrates with about 20 parts of ultrapure water and cleaned (10 minutes) using ultrasonic treatment.
2. The substrate surface is rinsed with ultrapure water for 3 minutes and then cleaned in ultrapure water (10 minutes) using ultrasonic treatment.
3. The substrate surface is rinsed with ultrapure water for 3 minutes again and then undergoes air drying.
4. The substrate undergoes UV ozonation (3 minutes).

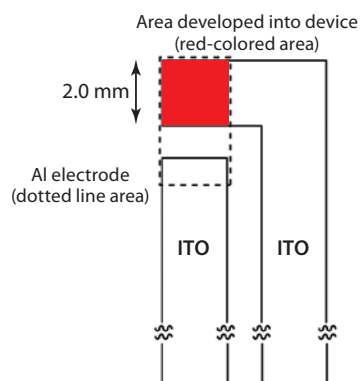


Figure 15. Example of ITO Patterning: constructing multiple patterns of this type on one substrate enables multiple devices to be simultaneously fabricated under the same conditions.

Solution Coating

The thickness of films obtained by the film formation depends upon the size of substrate used, the rotary speed of coaters, and the viscosity and boiling point, which depend on solvent used. The thickness of thin films formed under the same conditions as those of devices is evaluated. A stylus profile measuring system (Dektak) enables the film thickness in the solid state to be precisely measured. AFM may be substituted for Dektak.

The presence of insoluble elements and coagulation after the preparation of the solution results in defects in the formed film. Accordingly, it is essential to use filtration in advance to remove foreign matter from the solution. The filter used must be made of a material suitable for the solvent used (a material for water medium or for organic solvent) and have a pore diameter of about 0.45 μm.

1. Solution Coating of PEDOT:PSS

PEDOT:PSS is an aqueous dispersion where polystyrene sulfonate (PSS) is doped into poly(3,4-ethylenedioxythiophene) (PEDOT) to regulate ionization potential. In addition, PSS consists of colloidal nanoparticles with a diameter of 30 nm, so that application of its aqueous dispersion produces PEDOT:PSS layers with flat surfaces.

ITO glass is fixed on a spin coater, and several drops of PEDOT:PSS aqueous dispersion ([Aldrich Prod. No. 560596](http://aldrich.com/prod-no-560596)) are put on it and spread across the glass surface. Subsequently, spin coating is conducted at 1,500 to 3,000 rpm to form a PEDOT:PSS thin film with a thickness of 30 to 40 nm.

After the film formation, PEDOT:PSS in locations other than photoelectric conversion area is wiped off according to the ITO pattern by using a cotton swab or a spatula with a Kimwipes® wipe wrapped around it. Subsequently, the ITO glass undergoes heating treatment at 120 °C for 10 minutes to dry it. The above steps are followed under atmospheric conditions, and then the substrate is put under nitrogen in a glove box.

2. Solution Coating of Photoelectric Conversion Layer

Poly 3-hexylthiophene (P3HT) (Aldrich Prod. No. 698997; M_n 30,000–60,000) (15 mg) to be used as an electron donor, and PCBM (Aldrich Prod. No. 684457) (12 mg), to be used as an electron acceptor, are put into an amber vial in which chlorobenzene (1.0 mL) is then added to dissolve the two substances. Thus, a blend solution composed of about 1.25 wt% of P3HT and about 1.0 wt% of PCBM is prepared. This preparation may be conducted quickly outside the glove box, but after preparation, the vial must be put into the glove box under nitrogen and uncapped for nitrogen substitution.

The PEDOT:PSS-coated ITO glass substrate is heated at 180 °C for 5 minutes on a hot plate placed in the glove box for further drying and the elimination of oxygen. The substrate is fixed on a spin coater placed in the glove box. A P3HT:PCBM blend solution is filtered with a syringe filter (made of PTFE (polytetrafluoroethylene) and with a pore diameter of 0.45 μm) and put on the substrate to be spread by spin coating. A blend solution of this composition produces a thin film for a photoelectric conversion layer with a thickness of about 150 nm at a spin coating rotary speed of 1,500 rpm. At this point, the photoelectric layer is removed from the substrate in locations other than photoelectric conversion area.

If necessary, the substrate with the organic thin film is annealed. Annealing induces π - π stacking of thiophene frameworks between polymer chains in the π -conjugated polymer, so that the optical absorption and hole drift mobility properties are improved. Annealing treatments for such self-organization of polymers include heat treatment (thermal annealing) and solvent exposure treatment (solvent annealing). Although in heat treatment, self-organization progresses in a short time, the aggregation of fullerene derivatives occurs simultaneously and can interfere with the self-organization of polymers. On the other hand, solvent exposure treatment does not induce aggregation because the treatment is performed at room temperature; therefore, annealing takes longer compared with heat treatment. We conducted heat treatment (150 °C, 20 minutes) after deposition of the aluminum electrode.

Deposition of Aluminum Electrode

A deposition boat (molybdenum) on which aluminum is placed is put into a vacuum deposition apparatus connected to the glove box. The vacuum deposition apparatus is evacuated and then put under nitrogen, and subsequently the substrate is transferred from the glove box to the deposition chamber. Since the deposition chamber is connected with the glove box under nitrogen, the substrate can be placed in the deposition chamber completely without being exposed to the atmosphere. An electric current is applied to the deposition source under vacuum (up to 10^{-4} Pa) to heat the source, and an aluminum electrode is deposited while the deposition rate is controlled to be about 1 to 10 $\text{\AA}/\text{s}$ by using a quartz resonator thickness monitor that has undergone tooling until its thickness reaches 80 nm. Finally, nitrogen is injected in the deposition chamber, and the substrate is transferred to the glove box to be heated on the hot plate in the glove box for annealing.

Sealing

To prevent the device fabricated in the above manner from being exposed to the atmosphere, it is sealed by using a compact dispenser robot installed in the glove box. UV photo-setting resin is applied to the sealing glass, which is then added to the substrate. The resin-applied region is irradiated with UV light to adhere the sealing glass to the substrate in order to seal the device. The device characteristics of devices fabricated in this way can be evaluated under atmospheric conditions.

Evaluation of Device Characteristics

Measurement of current with voltage applied obtained from the device irradiated with light gives the following values: open-circuit voltage V_{oc} (V); short-circuit current density J_{sc} (mA/cm^2); fill factor FF (-); and power conversion efficiency PCE (%). Short-circuit current density must be commuted into the value per unit area where incident light is converted to electricity. A J-V curve and the relationship between the open-circuit voltage, the short-circuit current density, and the fill factor revealed from the measurement are shown below (Figure 16). The short-circuit current density is the current density that is obtained with no bias voltage applied. After this point, the open-circuit voltage is the voltage at which the current finally stops flowing when voltage is applied and increased in the direction opposing the current. There is a point where the product between current and voltage, that is, the output power, reaches its maximum on the segment of the J-V curve between the point representing the short-circuit current density J_{sc} and the point representing the open-circuit voltage V_{oc} .

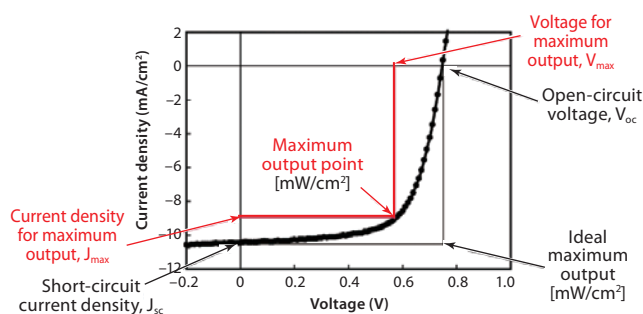


Figure 16. J-V curve and relationship between open-circuit voltage, short-circuit current density, and fill factor.

The current density and voltage at the maximum output are represented by J_{max} and V_{max} , respectively. The fill factor FF satisfies the following relationship.

$$FF = (J_{max} \times V_{max}) / (J_{sc} \times V_{oc})$$

In other words, FF is given by dividing the actual maximum output by the ideal maximum output ($J_{sc} \times V_{oc}$), which means that the characteristic is better when FF is closer to unity. Since the power conversion efficiency (PCE) is given by dividing the obtained electric energy (electric power) by the optical energy of incident light, the following equation holds when the energy of incident light is expressed as P_{inc} .

$$PCE (\%) = \{(J_{max} \times V_{max}) / P_{inc}\} \times 100$$

Evaluation during measurement is often done using a light source of $100 \text{ mW}/\text{cm}^2$. In this case, $P_{inc} = 100$, so that the following simple equation holds.

$$PCE (\%) = J_{max} \times V_{max} = V_{oc} \times J_{sc} \times FF$$

In evaluation, we used incident solar-simulated light (AM 1.5 G) ($100 \text{ mW}/\text{cm}^2$) from a solar simulator equipped with an air mass filter. The thickness of the atmosphere through which equatorial sunlight passes from directly above is regarded as AM 1.0, and at the latitude of Japan and nearby regions, sunlight is assumed to reach the ground after passing through atmosphere that is 1.5 times as thick. The J-V characteristic was measured with a sourcemeter unit (Keithley 2400 or similar). This sourcemeter unit may be substituted by a potentiostat (Hokuto Denko Corporation HZ-5000 or similar) used for electrochemical measurement, such as cyclic voltammetry (CV), and the results can be evaluated by linear sweep voltammetry (LSV).

In addition, spectral sensitivity in a wavelength region ranging from 350 to 750 nm was measured by irradiating the device with monochromatic light from a spectroscopy in the presence of bias light. The spectral sensitivity represents the ratio of the number of photons converted to electrons flowing through an external circuit to that of incident photons at each wavelength of light. To obtain the spectral sensitivity, the photoelectric current of the device was measured while the wavelength of the incident light was varied continuously.

According to the Japanese Industrial Standard JISC8931 (secondary reference amorphous solar cells), the amount of incident light is calibrated by using a standard solar cell. Thus, the light source used for the solar simulator is supposed to be calibrated by using a solar cell exhibiting a spectral characteristic similar to that of the solar cell to be evaluated. No reference cell for organic thin film solar cells is commercially available. Therefore, we evaluated the device performance by using a reference cell (Bunkoukeiki Co., Ltd. BS-520, a detector for amorphous silicon solar cells) to adjust the intensity of light from a light source lamp.

Actual Example of Device Characteristics

This section describes the characteristics of devices fabricated in accordance with the above manner, with P3HT used as the electron donor and PCBM or SIMEF used as the electron acceptor. The results of evaluating organic thin film solar cells using two different electron acceptors shows that the device using SIMEF produces higher V_{oc} (Figure 17), which reflects the characteristics of its higher LUMO level. Generally, J_{sc} declines for higher V_{oc} ; there often exists a trade-off between V_{oc} and J_{sc} . However, the device using SIMEF successfully increased V_{oc} without reducing J_{sc} . This is because of the ideal packing structure of SIMEF.

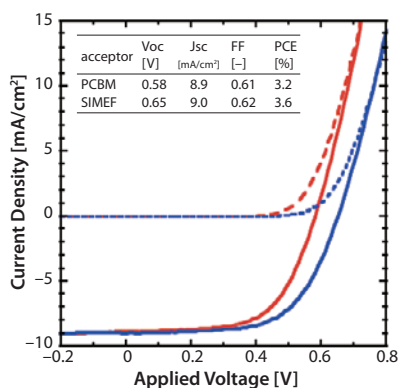


Figure 17. Device characteristics and J-V curve of organic thin film solar cell:
Solid lines: Photocurrent
Dotted lines: Dark current
Red lines: PCBM
Blue lines: SIMEF

There was no significant difference between the spectral sensitivity characteristics of the two devices (Figure 18), which accords with the fact that there was almost no difference in their short-circuit current density. Although the device using SIMEF showed a slightly higher IPCE, at around 450 nm, this was due to absorption by the fullerene derivative, that is, SIMEF. PCBM is a fullerene derivative with 1,2-type 58 π -electron systems, whereas SIMEF is a fullerene derivative with 1,4-type 58 π -electron systems; 1,4-adduct compounds absorb light at wavelengths near 450 nm.

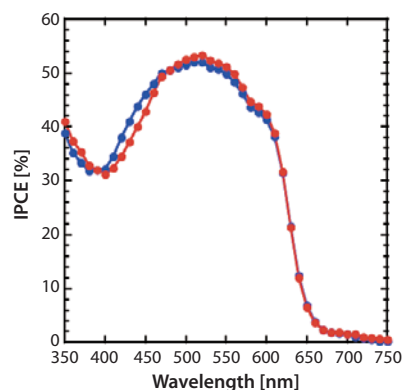


Figure 18. Spectral sensitivity spectra of organic thin film solar cells (IPCE: Incident Photon to Current Conversion Efficiency):
Red line: PCBM
Blue line: SIMEF

Conclusion

Organic thin film solar cells are made of organic compounds and characteristically form lightweight flexible solar cell products and can be print processed. These advantages enable us to design practical applications for them that are difficult to implement using silicon solar cells. Some have proposed applications such as mobile and outdoor battery chargers, indoor power generators, and specially designed building materials, although these are niche applications. As use of organic thin film solar cells spreads from a narrow niche field to the wider world and their conversion efficiency further improves, they will become applied to photovoltaic power generation for solving energy issues. The following challenges remain for widespread implementation of long-life highly efficient organic thin film solar cells.

1. Development of organic semiconductor materials that enable highly efficient light absorption and electron transfer
2. Construction of optimized molecular assembly and organization structures in organic thin films
3. Elucidation and precise construction of device structures that will produce highly efficient photoelectric conversion
4. Development of wide-area continuous coating processes for printing organic semiconductor molecules, such as roll-to-roll slot-dye coating, gravure printing, and ink-jet printing
5. Development of an inexpensive sealing process for high barrier properties

Acknowledgments

Some of the organic thin film solar cell data in this article were obtained in the ERATO Nakamura Functional Carbon Cluster Project of the Japan Science and Technology Agency. I am deeply grateful to Professor Eiichi Nakamura and Dr. Yoshiharu Sato, my collaborators in the Project. I am also very grateful to Mr. Naoki Obata for help in writing this article. The FET mobility of SIMEF in this article has been measured by Professor Zhenan Bao of Stanford University. I am grateful to Mitsubishi Chemical Corporation for supporting the foundation of the photoelectric conversion chemistry laboratory in School of Science of the University of Tokyo.

References

- (1) C. W. Tang, *Appl. Phys. Lett.* **1986**, *48*, 183.
- (2) H. W. Kroto, J. R. Heath, S. C. O'Brien, R. F. Curl, R. E. Smalley, *Nature* **1985**, *318*, 162.
- (3) D. Kearns, M. Calvin, *J. Chem. Phys.* **1958**, *29*, 950.
- (4) C. W. Tang, S. A. van Slyke, *Appl. Phys. Lett.* **1987**, *51*, 913.
- (5) M. Hiramoto, H. Fujiwara, M. Yokoyama, *Appl. Phys. Lett.* **1991**, *58*, 1062.
- (6) W. Kretschmer, L. Lamb, K. Fostiropoulos, D. Huffman, *Nature* **1990**, *347*, 354.
- (7) N. S. Sariciftci, L. Smilowitz, A. J. Heeger, F. Wudl, *Science* **1992**, *285*, 1474.
- (8) S. Morita, A. A. Zakhidov, K. Yoshino, *Solid State Commun.* **1992**, *82*, 249.
- (9) C. J. Brabec, G. Zerza, G. Cerullo, S. De Silvestri, S. Luzzatti, J. C. Hummelen, N. S. Sariciftci, *Chem. Phys. Lett.* **2001**, *340*, 232.
- (10) G. Yu, J. Gao, J. C. Hummelen, F. Wudl, A. J. Heeger, *Science* **1995**, *270*, 1789.
- (11) J. C. Hummelen, B. W. Knight, F. LePeq, F. Wudl, J. Yao, C. L. Wilkins, *J. Org. Chem.* **1995**, *60*, 532.
- (12) P. Schilinsky, C. Waldauf, C. J. Brabec, *Appl. Phys. Lett.* **2002**, *81*, 3885.
- (13) F. Padinger, F. R. S. Rittberger, N. S. Sariciftci, *Adv. Funct. Mater.* **2003**, *13*, 85.
- (14) G. Li, V. Shrotriya, J. Huang, Y. Yao, T. Moriarty, K. Emery, Y. Yang, *Nat. Mater.* **2005**, *4*, 864.
- (15) M. Reyes-Reyes, K. Kim, D. L. Carroll, *Appl. Phys. Lett.* **2005**, *87*, 83506.
- (16) Y. Kim, S. Cook, S. M. Tuladhar, S. A. Choulis, J. Nelson, J. R. Durrant, D. D. C. Bradley, M. Giles, I. McCulloch, C.-S. Ha, M. Ree, *Nat. Mater.* **2006**, *5*, 197.
- (17) D. Mülbacher, M. Scharber, M. Morana, Z. Zhu, D. Waller, R. Gaudiana, C. Brabec, *Adv. Mater.* **2006**, *18*, 2884.
- (18) J. Peet, J. Y. Kim, N. E. Coates, W. L. Ma, D. Moses, A. J. Heeger, G. C. Bazan, *Nat. Mater.* **2007**, *6*, 497.
- (19) J. Hou, H.-Y. Chen, S. Zhang, G. Li, Y. Yang, *J. Am. Chem. Soc.* **2008**, *130*, 16144.
- (20) Y. He, H.-Y. Chen, J. Hou, Y. Li, *J. Am. Chem. Soc.* **2010**, *132*, 1377.
- (21) Y. He, G. Zhao, B. Peng, Y. Li, *Adv. Funct. Mater.* **2010**, *20*, 3383.
- (22) G. Zhao, Y. He, Y. Li, *Adv. Mater.* **2010**, *22*, 4355.
- (23) Y.-J. Cheng, C.-H. Hsieh, Y. He, C.-S. Hsu, Y. Li, *J. Am. Chem. Soc.* **2010**, *132*, 17381.
- (24) J. Y. Kim, K. Lee, N. E. Coates, D. Moses, T.-Q. Nguyen, M. Dante, A. J. Heeger, *Science* **2007**, *317*, 222.
- (25) J. Y. Kim, S. H. Kim, H.-H. Lee, K. Lee, W. Ma, X. Gong, A. J. Heeger, *Adv. Mater.* **2006**, *18*, 572.
- (26) Y. Matsuo, A. Iwashita, Y. Abe, C.-Z. Li, K. Matsuo, M. Hashiguchi, E. Nakamura, *J. Am. Chem. Soc.* **2008**, *130*, 15429.
- (27) Y. Matsuo, Y. Sato, T. Niinomi, I. Soga, H. Tanaka, E. Nakamura, *J. Am. Chem. Soc.* **2009**, *131*, 16048.
- (28) M. Maggini, G. Scorrano, M. Prato, *J. Am. Chem. Soc.* **1993**, *115*, 9798.

PRODUCT HIGHLIGHT

Transparent Conductive Substrates

ITO Coated Slide

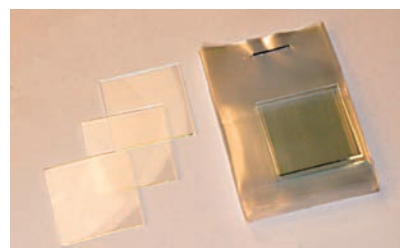
Thickness: 1.1 mm, surface resistivity: 8–12 Ω /sq

| | |
|--------------------------|------------------------------|
| rectangular (75 × 25 mm) | 578274-10PAK 578274-25PAK |
| square (25 × 25 mm) | 703192-10PAK |

Indium Oxide-coated PET Slide

Thickness: 0.2 mm, surface resistivity: 10 Ω /sq

| | |
|-----------------------|-----------------------------|
| square (150 × 150 mm) | 700177-5PAK 700177-10PAK |
|-----------------------|-----------------------------|

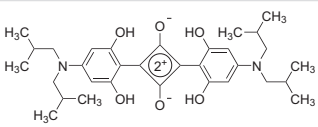
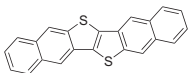
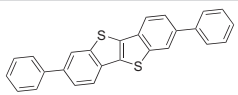
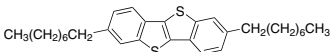
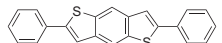
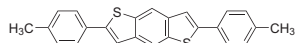
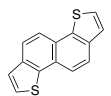
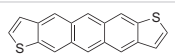
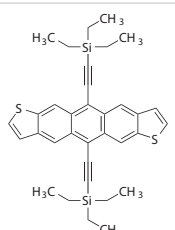
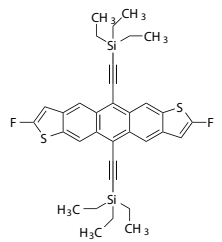
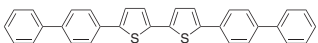
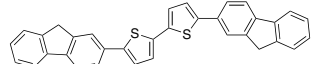
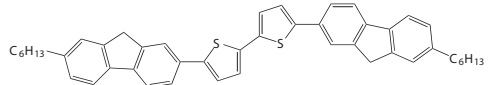
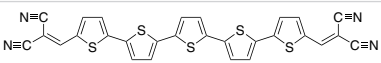
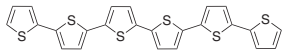
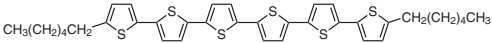


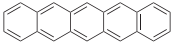
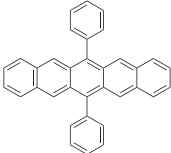
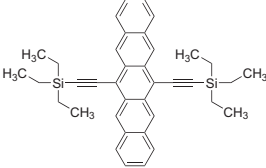
For a variety of substrates available from Sigma-Aldrich, visit sigma-aldrich.com/organelectronics

P-type Organic Semiconductors

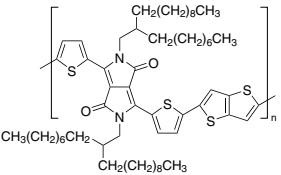
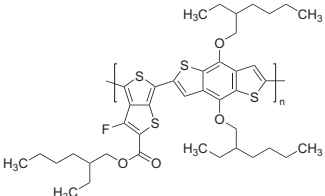
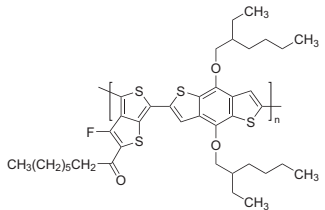
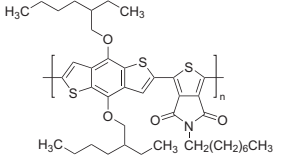
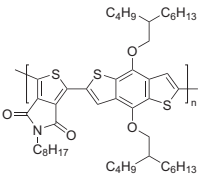
P-type Small Molecules

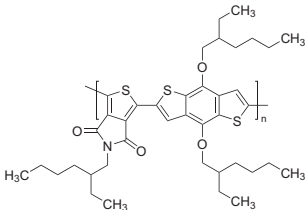
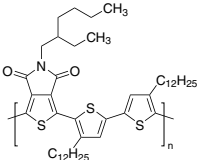
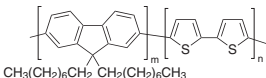
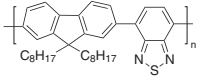
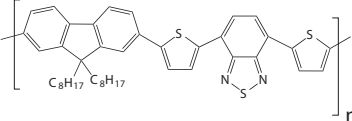
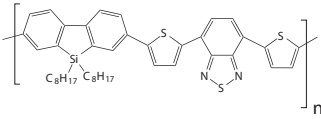
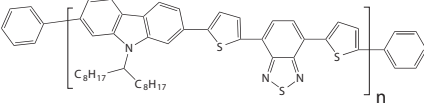
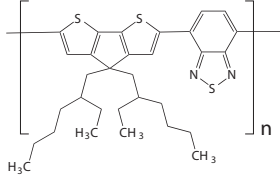
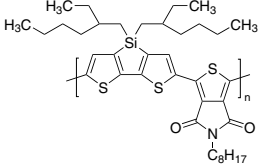
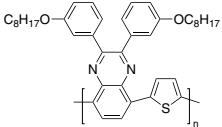
| Structure | Name | Optical Properties/Mobility | Purity | Prod. No. |
|-----------|---|---|-----------|--------------|
| | DTS(FBTTh ₂) ₂ | λ_{max} 590 nm in chloroform | - | 772380-100MG |
| | DTS(PTTh ₂) ₂ | λ_{max} 655 nm in chloroform | - | 772372-100MG |
| | 2-[(7-(5- <i>N,N</i> -Ditolyaminothiophen-2-yl)-2,1,3-benzothiadiazol-4-yl)methylene]malononitrile | λ_{abs} 662–664 nm in dichloro-methane | 99%, HPLC | 777293-250MG |
| | 2-[7-(4-Diphenylaminophenyl)-2,1,3-benzothiadiazol-4-yl)methylene]propanedinitrile | λ_{max} 549 nm in dichloro-methane | 96% | 790524-100MG |
| | 2-[(7-(4-(<i>N,N</i> -Bis(4-methylphenyl)amino)phenyl)-2,1,3-benzothiadiazol-4-yl)methylene]propanedinitrile | λ_{abs} 570 nm in dichloro-methane | 97%, HPLC | 777048-500MG |
| | SMDPPEH | λ_{abs} 644 nm in methylene chloride $\sim 10^{-4}$ cm ² /Vs | 97%, HPLC | 753912-250MG |
| | SMDPPO | λ_{abs} 644 nm in methylene chloride | - | 753920-250MG |
| | 2,4-Bis[4-(<i>N,N</i> -diphenylamino)-2,6-dihydroxyphenyl]suaraine | λ_{max} 720 nm | 98% | 757233-1G |
| | 2,4-Bis[4-(<i>N,N</i> -dibenzylamino)-2,6-dihydroxyphenyl]suaraine | λ_{max} 640–646 nm in chloroform | 97% | 757268-1G |

| Structure | Name | Optical Properties/Mobility | Purity | Prod. No. |
|---|---|---|---------------------|--|
|  | 2,4-Bis[4-(N,N-diisobutylamino)-2,6-dihydroxyphenyl] squaraine | λ_{max} 700 nm | 97% | 758337-1G |
|  | Dinaphtho[2,3-b:2',3'-f]thieno[3,2-b]thiophene | 2 cm ² /V·s | 99%, sublimed grade | 767638-100MG 767638-500MG |
|  | 2,7-Diphenyl[1]benzothieno[3,2-b][1]benzothiophene | 2 cm ² /V·s | 99%, sublimed grade | 767603-100MG 767603-500MG |
|  | C8-BTBT | 5.5 cm ² /V·s | ≥99%, HPLC | 747092-100MG 747092-250MG |
|  | 2,6-Diphenylbenzo[1,2-b:4,5-b']dithiophene | 4.6 × 10 ⁻³ cm ² /V·s | 97%, sublimed grade | 767611-100MG 767611-500MG |
|  | 2,6-Ditolybenzo[1,2-b:4,5-b']dithiophene | 10 ⁻² cm ² /V·s | 95%, sublimed grade | 767646-100MG 767646-500MG |
|  | Naphtho[1,2-b:5,6-b']dithiophene | >0.5 cm ² /V·s | 97% | 768677-500MG |
|  | ADT | 0.3 cm ² /V·s | 97% | 754080-250MG |
|  | TES-ADT | 1 cm ² /V·s | >99%, HPLC | 754102-100MG |
|  | diF-TES-ADT | 1 cm ² /V·s | 99%, HPLC | 754099-100MG |
|  | 5,5'-Di(4-biphenyl)-2,2'-bithiophene | 0.04 cm ² /V·s | 97% | 695947-1G |
|  | FTTF | 0.3 cm ² /V·s | sublimed grade | 754056-250MG |
|  | DH-FTTF | 0.05–0.12 cm ² /V·s | 95% | 754064-250MG |
|  | 5,5''-Bis(2''',2'''-dicyanovinyl)-2,2':5,2'':5'',5''':2''',5''''-quinquethiophene (DCVST) | λ_{abs} 530 nm in DMSO | ≥97% | 745596-250MG |
|  | α-Sexithiophene | 0.075 cm ² /V·s | - | 594687-1G |
|  | 5,5''-Dihexyl-2,2':5,2'':5'',5''':2''',5''''-sexithiophene | 0.13 cm ² /V·s | - | 633216-500MG |

| Structure | Name | Optical Properties/Mobility | Purity | Prod. No. |
|---|---|---|--|---|
|  | Pentacene | 0.4–3 cm ² /Vs | ≥99.995% trace metals basis, triple-sublimed grade | 698423-500MG |
| | Pentacene | 0.4–3 cm ² /Vs | ≥99.9% trace metals basis, sublimed grade | 684848-1G |
| | Pentacene | 0.4–3 cm ² /Vs | 99% | P1802-100MG P1802-1G P1802-5G |
|  | 6,13-Diphenylpentacene | UV absorption 308 nm in dichloromethane 8 × 10 ⁻⁵ cm ² /Vs | 98% | 760641-1G |
|  | 6,13-Bis((triethylsilyl)ethynyl)pentacene | 10 ⁻⁵ cm ² /Vs | ≥99%, HPLC | 739278-100MG 739278-500MG |

P-type Polymers

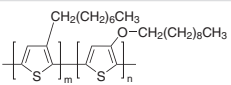
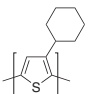
| Structure | Name | Molecular Weight | Optical Properties/Mobility | Prod. No. |
|---|--|---|--|------------------------------|
|  | PDPP2T-TT-OD | average M _w 40,000–60,000 by GPC | λ _{max} 820 nm | 791989-100MG |
|  | PTB7 | average M _w 80,000–200,000 | λ _{max} 680 nm | 772410-100MG |
|  | PBDTTT-CF | average M _w 53,000–83,000 by GPC | 7 × 10 ⁻⁴ cm ² /Vs | 772402-100MG |
|  | Poly[(5,6-dihydro-5-octyl-4,6-dioxo-4H-thieno[3,4-c]pyrrole-1,3-diy)]-[4,8-bis[(2-ethylhexyl)oxy]benzo-[1,2-b:4,5-b']dithiophene-2,6-diy]] | - | λ _{max} 627 nm | 773514-100MG |
|  | PBDTBO-TPDO | average M _n 10,000–50,000 | λ _{abs} 609, 557 nm in THF | 777080-100MG |

| Structure | Name | Molecular Weight | Optical Properties/Mobility | Prod. No. |
|---|--|-----------------------------------|--|--------------|
|  | PBDT-TPD | average M_n 10,000–50,000 | λ_{max} 608 nm | 776300-100MG |
|  | PBTPD | average M_n 3,500–20,000 g/mol | λ_{max} 572 nm | 745901-100MG |
|  | Poly[(9,9-dioctylfluorenyl-2,7-diyl)-co-bithiophene] | average M_n >20,000 | λ_{em} = 497 nm in chloroform (at M_n = 20,000) $5 \times 10^{-3} \text{ cm}^2/\text{V}\cdot\text{s}$ | 685070-250MG |
|  | Poly[(9,9-di-n-octylfluorenyl-2,7-diyl)-alt-(benzo[2,1,3]thiadiazol-4,8-diyl)] | average M_n 10,000–20,000 | λ_{em} = 515–535 nm in chloroform $4 \times 10^{-3} \text{ cm}^2/\text{V}\cdot\text{s}$ | 698687-250MG |
|  | PFO-DBT | average M_w 10,000–50,000 | $3 \times 10^{-4} \text{ cm}^2/\text{V}\cdot\text{s}$ | 754013-100MG |
|  | PSiF-DBT | M_n 10,000–80,000 | $10^{-3} \text{ cm}^2/\text{V}\cdot\text{s}$ | 754021-100MG |
|  | PCDTBT | - | λ_{max} 576 nm $6 \times 10^{-5} \text{ cm}^2/\text{V}\cdot\text{s}$ | 753998-100MG |
|  | PCPDTBT | average M_w 7,000–20,000 | λ_{max} 700 nm $2 \times 10^{-2} \text{ cm}^2/\text{V}\cdot\text{s}$ | 754005-100MG |
|  | PDTSTPD | average M_n 7,000–35,000 by GPC | λ_{max} 670 nm $1.0 \times 10^{-4} \text{ cm}^2/\text{V}\cdot\text{s}$ | 745928-100MG |
|  | TQ1 | M_n 12,000–45,000 g/mol | λ_{max} 620 nm | 745898-100MG |

| Structure | Name | Molecular Weight | Optical Properties/Mobility | Prod. No. |
|-----------|--|----------------------------------|--|---|
| | Poly[2-methoxy-5-(2-ethylhexyloxy)-1,4-phenylenevinylene] | average M_n 40,000–70,000 | λ_{em} = 554 nm in toluene | 541443-250MG 541443-1G |
| | Poly[2-methoxy-5-(2-ethylhexyloxy)-1,4-phenylenevinylene] | average M_n 70,000–100,000 | λ_{em} = 554 nm in toluene | 541435-1G |
| | Poly[2-methoxy-5-(2-ethylhexyloxy)-1,4-phenylenevinylene] | average M_n 150,000–250,000 | λ_{em} = 554 nm in toluene | 536512-1G |
| | Poly[2-methoxy-5-(3,7'-dimethyloxyloxy)-1,4-phenylenevinylene] | M_n ~120,000 | λ_{em} = 555 nm in toluene | 546461-250MG 546461-1G |
| | Poly[bis(4-phenyl)(2,4,6-trimethylphenyl)amine] | average M_n 7,000–10,000 (GPC) | 10^{-3} - 10^{-2} cm ² /V·s | 702471-100MG 702471-1G |

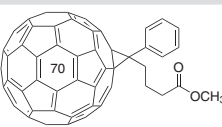
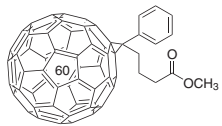
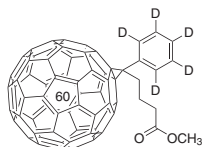
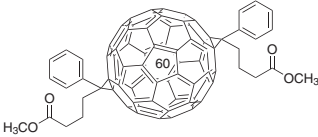
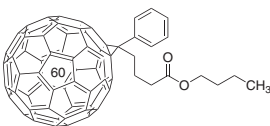
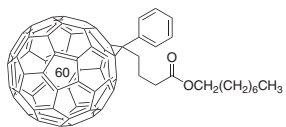
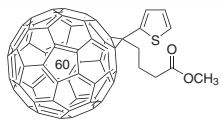
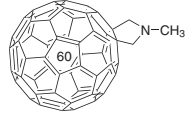
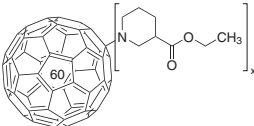
Polythiophenes (PT)


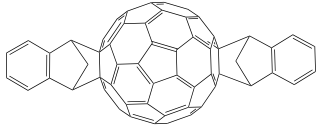
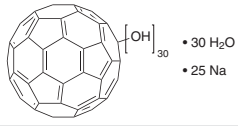
| Name | Structure | Regioregularity | Mol. Wt. | Prod. No. |
|-----------------------------------|-----------|-----------------|--|--|
| Poly(3-butylthiophene-2,5-diyl) | | regioregular | M_w 54,000 (typical) | 495336-1G |
| Poly(3-butylthiophene-2,5-diyl) | | regiorandom | - | 511420-1G |
| Poly(3-hexylthiophene-2,5-diyl) | | regioregular | average M_n 54,000–75,000 | 698997-250MG 698997-1G 698997-5G |
| Poly(3-hexylthiophene-2,5-diyl) | | regioregular | average M_n 15,000–45,000 | 698989-250MG 698989-1G 698989-5G |
| Poly(3-hexylthiophene-2,5-diyl) | | regioregular | - | 445703-1G |
| Poly(3-hexylthiophene-2,5-diyl) | | regiorandom | - | 510823-1G |
| Poly(3-octylthiophene-2,5-diyl) | | regioregular | M_n ~34,000 | 445711-1G |
| Poly(3-octylthiophene-2,5-diyl) | | regioregular | average M_n ~25,000 | 682799-250MG |
| Poly(3-dodecylthiophene-2,5-diyl) | | regioregular | average M_n ~30,000 average M_w ~42,000 | 495344-1G |
| Poly(3-dodecylthiophene-2,5-diyl) | | regioregular | average M_w ~60,000 | 450650-1G |
| Poly(3-dodecylthiophene-2,5-diyl) | | regioregular | average M_w ~27,000 | 682780-250MG |

| Name | Structure | Regioregularity | Mol. Wt. | Prod. No. |
|---|---|-----------------|---|------------------------------|
| Poly(3-octylthiophene-2,5-diyl-co-3-decyloxythiophene-2,5-diyl) |  | - | M _n 8,000 M _w 21,000 | 696897-250MG |
| Poly(3-cyclohexylthiophene-2,5-diyl) |  | - | - | 557625-1G |

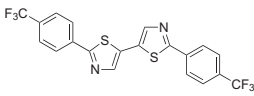
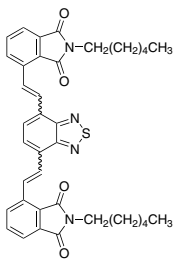
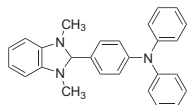
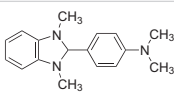
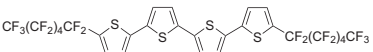
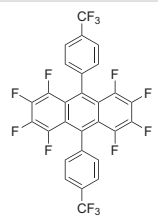
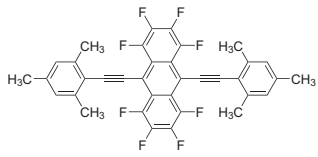
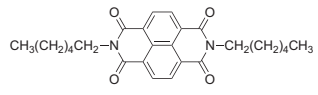
N-type Organic Semiconductors

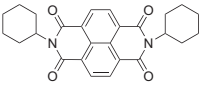
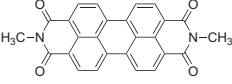


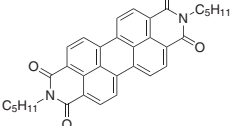
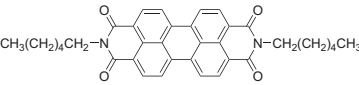

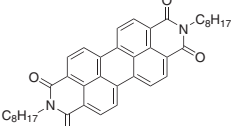
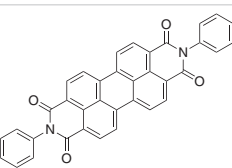
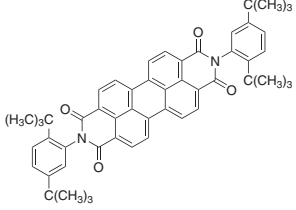
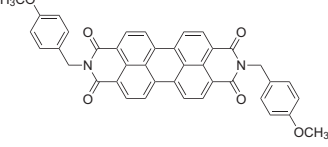

Fullerenes

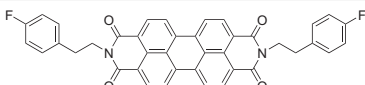

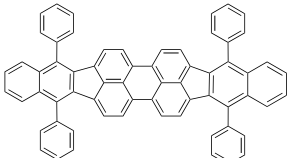
| Structure | Name | Purity | Prod. No. |
|---|---|----------------------|--|
|  | [6,6]-Phenyl C ₇₁ butyric acid methyl ester, mixture of isomers | 99% | 684465-100MG 684465-500MG |
|  | [6,6]-Phenyl C ₆₁ butyric acid methyl ester | >99.9% | 684457-100MG |
| | [6,6]-Phenyl C ₆₁ butyric acid methyl ester | >99.5% | 684449-100MG 684449-500MG |
| | [6,6]-Phenyl C ₆₁ butyric acid methyl ester | >99% | 684430-1G |
|  | [6,6]-Pentadeuterophenyl C ₆₁ butyric acid methyl ester | 99.5% | 684503-100MG |
|  | [6,6] Diphenyl C ₆₂ bis(butyric acid methyl ester)(mixture of isomers) | 99.5% | 704326-100MG |
|  | [6,6]-Phenyl-C ₆₁ butyric acid butyl ester | >97% | 685321-100MG 685321-1G |
|  | [6,6]-Phenyl-C ₆₁ butyric acid octyl ester | ≥99% | 684481-100MG |
|  | [6,6]-Thienyl C ₆₁ butyric acid methyl ester | ≥99% | 688215-100MG |
|  | N-Methylfulleropyrrolidine | 99%, HPLC | 668184-100MG |
|  | Small gap fullerene-ethyl nipecotate | ≥95%, fullerenes 50% | 707473-250MG |

| Structure | Name | Purity | Prod. No. |
|---|--|-----------------------------|--------------|
|  | ICMA | 97%, HPLC | 753947-250MG |
|  | ICBA | 99%, HPLC | 753955-250MG |
|  | Polyhydroxy small gap fullerenes, hydrated | Polyhydroxy SGFs(TGA) ~ 85% | 707481-100MG |

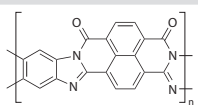
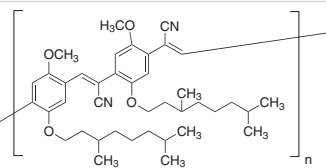
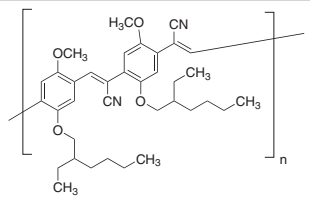
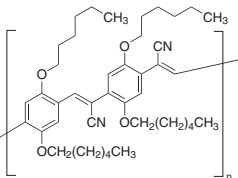
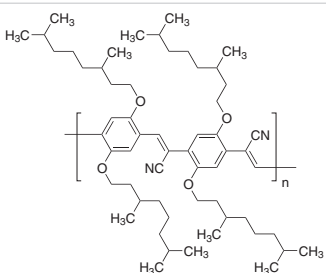
N-type Small Molecules

| Structure | Name | Optical Properties/Mobility | Purity/Dye Content | Prod. No. |
|---|---|---|--------------------|---------------------------|
|  | 2,2'-Bis[4-(trifluoromethyl)phenyl]-5,5'-bithiazole | 1.83 cm ² /V·s | 97% | 749257-500MG |
|  | PI-BT | λ_{max} 448 nm in THF | >97% | 790893-250MG 790893-1G |
|  | 4-(1,3-Dimethyl-2,3-dihydro-1H-benzoimidazol-2-yl)-N,N-diphenylamine | λ_{abs} 308 nm in dichloromethane | 98% | 767321-1G |
|  | 4-(2,3-Dihydro-1,3-dimethyl-1H-benzimidazol-2-yl)-N,N-dimethylbenzenamine | - | 98%, HPLC | 776734-1G |
|  | 5,5''-Bis(tridecafluorohexyl)-2,2':5':2'':5'2''-quaterthiophene | ≤ 0.64 cm ² /V·s | - | 764639-250MG 764639-1G |
|  | 1,2,3,4,5,6,7,8-Octafluoro-9,10-bis[4-(trifluoromethyl)phenyl]anthracene | - | 97% | 757179-1G |
|  | 1,2,3,4,5,6,7,8-Octafluoro-9,10-bis[2-(2,4,6-trimethylphenyl)ethynyl]anthracene | - | 97% | 758442-250MG |
|  | 2,7-Dihexylbenzo[1,3,6,8]phenanthroline-1,3,6,8(2H,7H)-tetrone | λ_{abs} 380, 360, 342 nm in dichloromethane 0.7 cm ² /V·s | - | 768464-500MG |

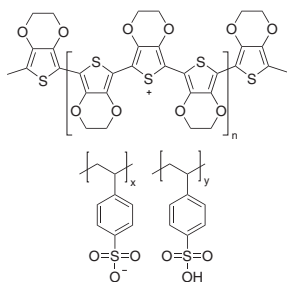
| Structure | Name | Optical Properties/Mobility | Purity/Dye Content | Prod. No. |
|---|--|--|-------------------------|--------------------------------------|
|  | 1,3,6,8(2H,7H)-Tetraone, 2,7-dicyclohexylbenzo[Imn][3,8]phenanthroline | λ_{abs} 382, 362, 243 nm in chloroform $6 \text{ cm}^2/\text{V}\cdot\text{s}$ | 98% | 761443-1G |
|  | <i>N,N'</i> -Dimethyl-3,4,9,10-perylenedicarboximide | λ_{abs} 522 nm in dichloromethane $10^{-5} \text{ cm}^2/\text{V}\cdot\text{s}$ | 98% | 771481-1G 771481-5G |
|  | 2,9-Dipropylantra[2,1,9-def6,5,10-d'e'f']diisoquinoline-1,3,8,10(2H,9H)tetrone | λ_{abs} 524, 488 nm $0.1\text{-}2.1 \text{ cm}^2/\text{V}\cdot\text{s}$ | 97% | 771635-1G |
|  | <i>N,N'</i> -Bis(3-pentyl)perylene-3,4,9,10-bis(dicarboximide) | λ_{abs} 524, 488, 457 nm in dichloromethane | 99%, HPLC | 776289-1G |
|  | <i>N,N'</i> -Dipentyl-3,4,9,10-perylenedicarboximide | λ_{max} 527 nm $\sim 10^{-4} \text{ cm}^2/\text{V}\cdot\text{s}$ | 98% | 663921-500MG |
|  | 2,9-Dihexylantra[2,1,9-def6,5,10-d'e'f']diisoquinoline-1,3,8,10(2H,9H)tetrone | λ_{abs} 524, 448, 229 nm in dichloromethane $0.1\text{-}2.1 \text{ cm}^2/\text{V}\cdot\text{s}$ | 98% | 773816-1G |
|  | 2,9-Diheptylantra[2,1,9-def6,5,10-d'e'f']diisoquinoline-1,3,8,10(2H,9H)tetrone | λ_{max} 254 nm in dichloromethane $1.4 \times 10^{-2} \text{ cm}^2/\text{V}\cdot\text{s}$ | 99% | 773824-1G |
|  | <i>N,N'</i> -Dioctyl-3,4,9,10-perylenedicarboximide | λ_{max} 526 nm $1.7 \text{ cm}^2/\text{V}\cdot\text{s}$ | 98% | 663913-1G |
|  | <i>N,N'</i> -Diphenyl-3,4,9,10-perylenedicarboximide | λ_{max} 527 nm $10^{-5} \text{ cm}^2/\text{V}\cdot\text{s}$ | 98% | 663905-500MG |
|  | <i>N,N'</i> -Bis(2,5-di- <i>tert</i> -butylphenyl)-3,4,9,10-perylenedicarboximide | λ_{max} 528 nm $1.8 \times 10^{-4} \text{ cm}^2/\text{V}\cdot\text{s}$ | Dye content 97% | 264229-100MG |
|  | 2,9-Bis[(4-methoxyphenyl)methyl]antra[2,1,9-def6,5,10-d'e'f']diisoquinoline-1,3,8,10(2H,9H)tetrone | λ_{abs} 527, 490 nm in dichloromethane $0.5 \text{ cm}^2/\text{V}\cdot\text{s}$ | 99% | 771627-1G |
|  | 1,3,8,10(2H,9H)-Tetraone, 2,9-bis(2-phenylethyl)antra[2,1,9-def6,5,10-d'e'f']diisoquinoline | $1.4 \text{ cm}^2/\text{V}\cdot\text{s}$ | 98%, elemental analysis | 761451-1G |

| Structure | Name | Optical Properties/Mobility | Purity/Dye Content | Prod. No. |
|---|--|-----------------------------|--------------------|------------------------------|
|  | 2,9-Bis[2-(4-fluorophenyl)ethyl]anthra[2,1,9-def,6,5,10-d'e'f']diisoquinoline-1,3,8,10(2H,9H)tetrone | - | 95% | 763942-1G |
|  | 2,9-Bis[2-(4-chlorophenyl)ethyl]anthra[2,1,9-def,6,5,10-d'e'f']diisoquinoline-1,3,8,10(2H,9H)tetrone | - | 98% | 767468-1G |
|  | DBP | - | 98%, HPLC | 753939-250MG |

N-type Polymers

| Structure | Name | Mobility | Prod. No. |
|---|--|---------------------------------------|---|
|  | Poly(benzimidazobenzophenanthroline) | 0.1 cm ² /Vs | 667846-250MG 667846-1G |
|  | Poly(5-(3,7-dimethyloxy)-2-methoxy-cyanoterephthalylidene) | ~10 ⁻⁵ cm ² /Vs | 646628-250MG |
|  | Poly(5-(2-ethylhexyloxy)-2-methoxy-cyanoterephthalylidene) | ~10 ⁻⁵ cm ² /Vs | 646644-250MG |
|  | Poly(2,5-di(hexyloxy)cyanoterephthalylidene) | ~10 ⁻⁵ cm ² /Vs | 646652-250MG |
|  | Poly(2,5-di(3,7-dimethyloxy)cyanoterephthalylidene) | ~10 ⁻⁵ cm ² /Vs | 646571-250MG |

PEDOT:PSS



| Description | Sheet Resistance (Ω/sq) | Viscosity | pH | Prod. No. |
|--|---|------------------------------|--------------------------------------|---|
| dry re-dispersible pellets | 200–450 | n/a | - | 768618-1G 768618-5G |
| 1.0 wt. % in H_2O | 50–120 | 7–12 mPa.s at 22 °C | 1.8–2.2 | 768642-25G |
| 5.0 wt. %, conductive screen printable ink | 50–150 | 50,000–90,000 mPa.s at 22 °C | 1.5–2.0 | 768650-25G |
| 0.8% in H_2O , conductive inkjet ink | - | 7–12 cP at 22 °C | 1.5–2.5 | 739316-25G |
| 1.1% in H_2O , neutral pH | <100 (>70% visible light transmission, 40 μm wet) | <100 cP at 22 °C | 5–7 | 739324-100G |
| 1.1% in H_2O , surfactant-free | <100 (<80% visible light transmission, 40 μm wet) | <100 cP at 22 °C | <2.5 | 739332-100G |
| 0.54% in H_2O | <200 (>90% visible light transmission, 40 μm wet) | <18 cP at 22 °C | <2.7 | 739340-25G 739340-100G |
| 3.0-4.0% in H_2O | 1,500 (4 point probe measurement of dried coating based on initial 6 μm wet thickness.) 500 (4 point probe measurement of dried coating based on initial 18 μm wet thickness.) | 10–30 cP at 20 °C | 1.5–2.5 at 25 °C (dried coatings) | 655201-5G 655201-25G |
| 2.8 wt % dispersion in H_2O | - | <20 cP at 20 °C | 1.2–1.8 | 560596-25G 560596-100G |

Indium Tin Oxide (ITO) Coated Substrates

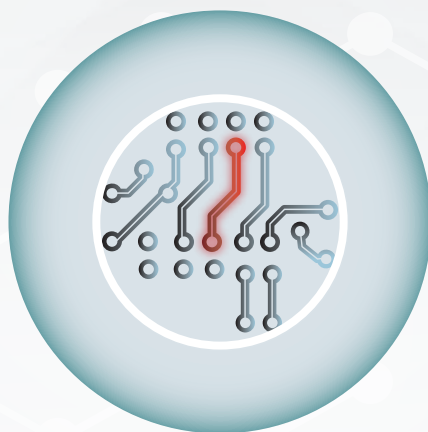
| Description | L x W x Thickness (mm) | Surface Resistivity (Ω/sq) | Prod. No. |
|--|------------------------|--|--|
| Indium tin oxide coated PET | 1 ft x 1 ft x 5 mil | 60 | 639303-1EA 639303-5EA |
| | 1 ft x 1 ft x 5 mil | 100 | 639281-1EA 639281-5EA |
| | 1 ft x 1 ft x 5 mil | 200 | 749745-1EA 749745-5EA |
| | 1 ft x 1 ft x 5 mil | 250 | 749761-1EA 749761-5EA |
| | 1 ft x 1 ft x 5 mil | 300 | 749796-1EA 749796-5EA |
| | 1 ft x 1 ft x 7 mil | 60 | 749729-1EA 749729-5EA |
| | 1 ft x 1 ft x 7 mil | 100 | 749737-1EA 749737-5EA |
| | 1 ft x 1 ft x 7 mil | 200 | 749753-1EA 749753-5EA |
| | 1 ft x 1 ft x 7 mil | 250 | 749788-1EA 749788-5EA |
| | 1 ft x 1 ft x 7 mil | 300 | 749818-1EA 749818-5EA |
| Indium tin oxide coated glass slide, square | 25 x 25 x 1.1 | 8–12 | 703192-10PAK |
| | 25 x 25 x 1.1 | 30–60 | 703184-10PAK |
| | 25 x 25 x 1.1 | 70–100 | 703176-10PAK |
| Indium tin oxide coated glass slide, rectangular | 75 x 25 x 1.1 | 8–12 | 578274-10PAK 578274-25PAK |
| | 75 x 25 x 1.1 | 15–25 | 636916-10PAK 636916-25PAK |
| | 75 x 25 x 1.1 | 30–60 | 636908-10PAK 636908-25PAK |
| | 75 x 25 x 1.1 | 70–100 | 576352-10PAK 576352-25PAK |
| | 75 x 25 x 1.1 | 5–15 | 576360-10PAK 576360-25PAK |

MATERIALS TO DRIVE INNOVATION



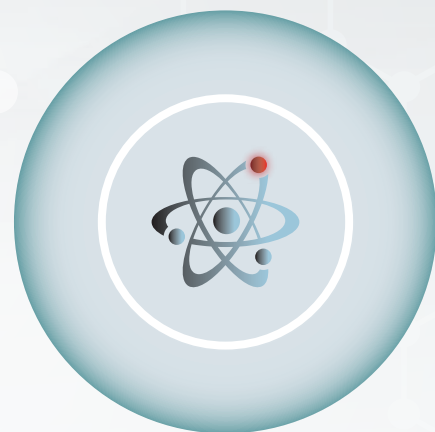
BIOMEDICAL

- Materials for drug delivery, bone and tissue engineering
- PEGs, biodegradable and natural polymers
- Functionalized nanoparticles
- Block copolymers and dendrimers
- Nanoclays



ELECTRONICS

- Nanowires
- Printed electronics inks and pastes
- Materials for OPV, OFET and OLED
- Nanodispersions
- CNTs and graphene
- Precursors for PVD, CVD and sputtering



ENERGY

- Electrode and electrolyte materials for batteries and fuel cells
- Hydrogen storage materials, including MOFs
- Phosphors
- Thermoelectrics
- Nanomaterials
- Precursors for nanomaterials and nanocomposites

Find more information on our capabilities at
aldrich.com/matsci

*Enabling Science to
Improve the Quality of Life*

Order/Customer Service: sigma-aldrich.com/order
Technical Service: sigma-aldrich.com/techservice
Development/Custom Manufacturing Inquiries **SAFC** safcglobal@sial.com
Safety-related Information: sigma-aldrich.com/safetycenter

World Headquarters
3050 Spruce St.
St. Louis, MO 63103
(314) 771-5765
sigma-aldrich.com